



## Salt-induced crestal faults control the formation of Quaternary tunnel valleys in the southern North Sea

STEFAN WENAU AND TIAGO M. ALVES

BOREAS



Wenau, S. & Alves, T. M.: Salt-induced crestal faults control the formation of Quaternary tunnel valleys in the southern North Sea. *Boreas*. <https://doi.org/10.1111/bor.12461>. ISSN 0300-9483.

Tunnel valleys are major features of glaciated margins and they enable meltwater expulsion from underneath a thick ice cover. Their formation is related to the erosion of subglacial sediments by overpressured meltwater and direct glacial erosion. Yet, the impact of pre-existing structures on their formation and morphology remains poorly known. High-quality 3D seismic data allowed the mapping of a large tunnel valley that eroded underlying preglacial delta deposits in the southern North Sea. The valley follows the N–S strike of crestal faults related to a Zechstein salt wall. A change in downstream tunnel valley orientation towards the SE accompanies a change in the strike direction of salt-induced faults. Fault offsets indicate important activity of crestal faults during the deposition of preglacial deltaic sediments. We propose that crestal faults facilitated tunnel valley erosion by acting as high-permeability pathways and allowing subglacial meltwater to reach low-permeability sediments in the underlying Neogene deltaic sequences, ultimately resulting in meltwater overpressure build-up and tunnel valley excavation. Active faults probably also weakened the near-surface sediment to allow a more efficient erosion of the glacial substrate. This control of substrate structures on tunnel valley morphology is considered as a primary factor in subglacial drainage pattern development in the study area.

*Stefan Wenau (swenau@uni-bremen.de), Department of Geosciences, University of Bremen, Klagenfurter Str. 2-4, 28359 Bremen Germany and Fraunhofer IWES, Fraunhofer Institute for Wind Energy Systems, Am Fallturm 5, 28359 Bremen, Germany; Tiago M. Alves, 3D Seismic Lab, School of Earth and Ocean Sciences, Cardiff University, Main Building-Park Place, Cardiff CF10 3AT, UK; received 19th November 2019, accepted 4th June 2020.*

Tunnel valleys are a common feature in glacial environments as thoroughly documented in Quaternary deposits of northern Europe (e.g. Huuse & Lykke-Andersen 2000; Van der Vegt *et al.* 2012), North America (e.g. Cutler *et al.* 2002; Kehew *et al.* 2012) and in Palaeozoic successions around the world (e.g. Ghienne *et al.* 2003; Ravier *et al.* 2014). Tunnel valleys are deep V- or U-shaped erosional features often incised below a regional base level; they have straight or slightly meandering courses, steep flanks, and abrupt terminations (Van der Vegt *et al.* 2012 and references therein). Their formation is generally due to overpressured subglacial meltwater eroding the underlying substrate, acting in tandem with direct glacial erosion to form deep valleys running parallel to the direction of ice advance (Ó Cofaigh 1996; Huuse & Lykke-Andersen 2000; Jørgensen & Sandersen 2006; Van der Vegt *et al.* 2012).

Recent studies have considered the combined effect of ice loading and subglacial meltwater on pore-water pressure, associated fracturing and subglacial sediment fluidization, key physical processes that result in the formation of tunnel valleys (Janszen *et al.* 2012; Sandersen & Jørgensen 2012; Ravier *et al.* 2014; Lelandais *et al.* 2016). The varying resistance to erosion of subglacial sediments generates deep valleys in sandy deposits, smaller valleys in chalky sediments and eskers on crystalline basement (Boulton *et al.* 2009; Moreau *et al.* 2012). In contrast, subglacial pore-water pressure was reported to facilitate enhanced tunnel valley formation in fine-grained, low-permeability sediments (Janszen *et al.* 2012). The published data also suggest

that salt structures can control the course of tunnel valleys either by guiding them (Piotrowski 1997) or diverting their formation (Kristensen *et al.* 2007). Underlying faults affect tunnel valleys, aligning them with main fault zones (Dobracki & Krzyszkowski 1997; Ghienne *et al.* 2003; Ravier *et al.* 2014), but similar effects may also be due to pre-existing valleys being re-occupied by new ones (Stewart *et al.* 2012). Hence, it remains unclear how exactly the pre-existing structures influence tunnel valley formation, their courses and morphology.

This study investigates a large tunnel valley in the southern North Sea and its relationship to underlying salt-induced faults. A high-quality 3D seismic volume from the Broad Fourteens Basin is used to investigate the presence of faults below a Quaternary tunnel valley system. This work aims to address (i) how crestal faults of rising diapirs control tunnel valley erosion in an area of the southern North Sea, (ii) how the morphology of tunnel valleys varies in relation to the underlying structures, and (iii) how secondary tunnel valleys vary in size, depth and orientation adjacent to a major tunnel valley.

### Data and methods

This study is based on a 3D seismic volume with an area of ~842 km<sup>2</sup> acquired over the Broad Fourteens Basin, in the Dutch sector of the southern North Sea (Fig. 1). The data set is used for the interpretation of Cenozoic successions in the area (Fig. 2). The seismic data are

zero-phased with a dominant frequency of  $\sim 40$  Hz (Figs 3–6). They are part of a seismic survey acquired in the late 2000s and processed with a focus on deep sub-Zechstein (i.e. sub-salt) reservoirs. Seismic interpretation was carried out using Schlumberger's Petrel (R).

A total of 34 boreholes are tied to the interpreted seismic volume (Fig. 1). Velocity ( $V_p$ ) data are provided with the borehole lithological descriptions (Fig. 3). These  $V_p$  data are tied to discrete seismic reflections, revealing a minimum tuning thickness ( $\lambda/4$ ) of  $\sim 15$  m at the depth of the faults and tunnel valleys interpreted in this work. Such a seismic resolution approaches the maximum resolution ( $\lambda/30$ , or  $\sim 6$ – $7$  m) expected by seismic data imaging of the uppermost Miocene–Quaternary strata. The bin spacing of the seismic data is  $25 \times 25$  m, while its sampling interval is 4 ms.

Very shallow sediments reveal a loss in seismic resolution at depths shallower than  $\sim 200$  ms two-way travel time (TWT), particularly close to the sea floor (Figs 3–6). Nevertheless, the imaging quality of the seismic data is sufficient to map faults through to the sea floor and identify tunnel valley shoulders within glacial sediment (Fig. 6). The imaging quality is very good at a depth of  $\sim 300$ – $600$  ms TWT, the main focus of this study, allowing a detailed interpretation of geological structures.

The interpreted 3D seismic volume shows a number of data gaps due to the presence of offshore platforms in the study area, which had to be avoided by the acquisition vessel, but these gaps do not significantly affect the

interpretation of the data (Figs 4, 7, 8). A minor acquisition footprint in a NE–SW direction is visible on some of the mapped horizons (Fig. 8B).

Several exploration wells drilled through the Quaternary glacial deposits to reveal an essentially sandy-silty succession over mudstone units of Palaeogene age (Fig. 2). These exploration wells were used to tie our seismic data to regional stratigraphical units. In total, five horizons (H1 to H5) were interpreted to investigate the geological evolution of the study area in the Cenozoic and, especially, during the Pleistocene (Figs 2–6). In addition, variance time slices and horizon maps were used to map salt-induced faults in the upper part of the sedimentary column in relation to tunnel valley courses (Figs 7, 8).

Pull-up or push-down effects caused by anomalous  $V_p$  velocities in tunnel-valley fills, as observed in other studies (e.g. Kristensen & Huuse 2012), were not found in our data. Seismic reflections beneath the tunnel valleys do not show systematic distortions caused by velocity effects (e.g. Figs 5, 6). Similarly, fault offsets are clearly visible along discrete seismic reflectors independently from their location below or adjacent to tunnel valleys (e.g. Fig. 5).

## Geological setting

The Dutch sector of the southern North Sea has undergone a complex geological evolution since the

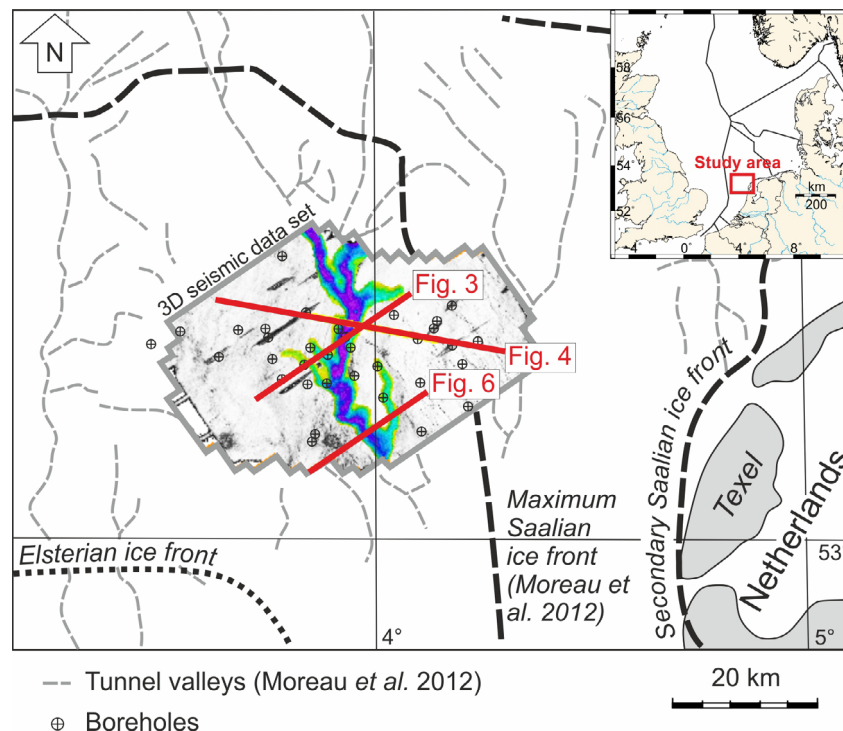


Fig. 1. Overview map of the study area of the southern North Sea. Mapped tunnel valleys and ice fronts are the main glacial features (Laban 1995; Praeg 1996; Gibbard *et al.* 2009; Moreau *et al.* 2012). The data set is situated in the area primarily affected by the Elsterian ice sheet. Boreholes available for stratigraphical ties to the seismic data are indicated. Colour-coded time structure is the mapped major tunnel valley (Fig. 7B).

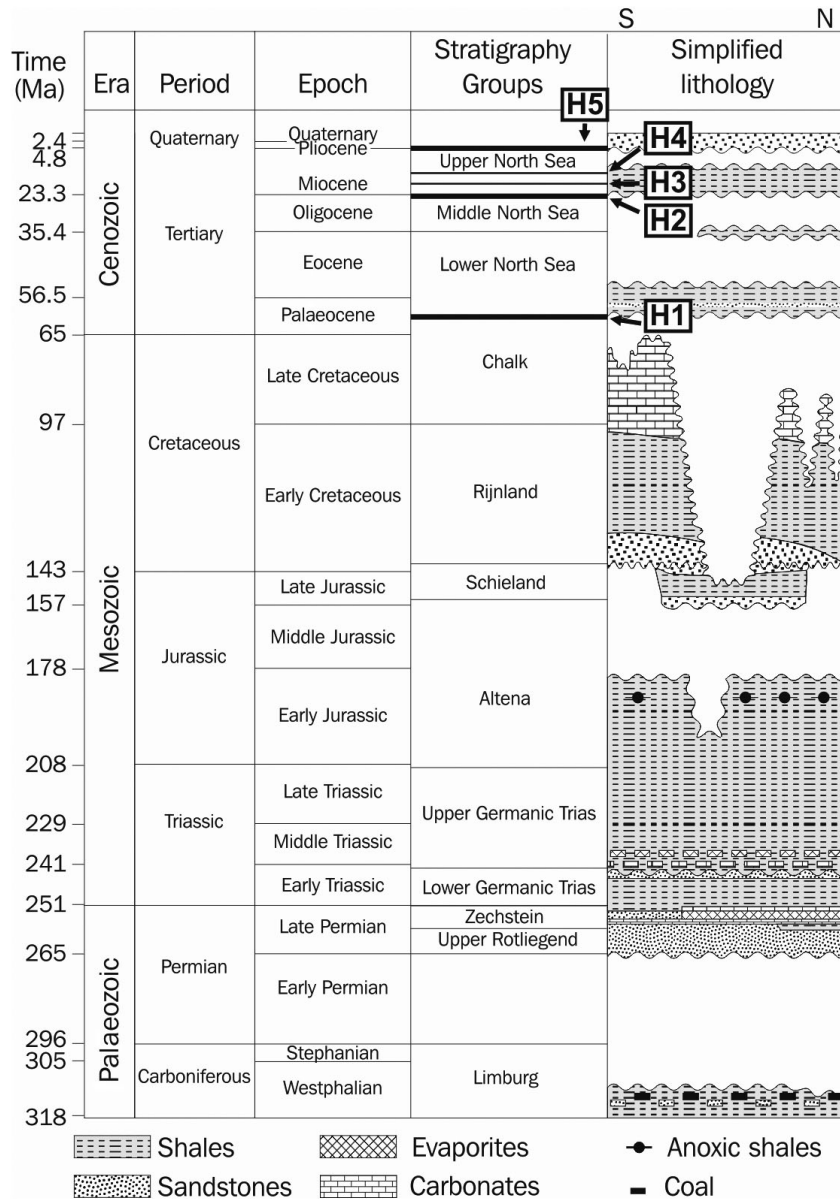


Fig. 2. Simplified stratigraphical column of the Dutch sector of the southern North Sea (modified from Penge *et al.* 1999; Verweij & Simmelink 2002; Alves & Elliott 2014). The horizons mapped represent the main Cenozoic seismic-stratigraphical markers in the Broad Fourteens Basin.

Carboniferous, recording continental rifting, tectonic inversion and widespread halokinesis (Van Wijhe 1987; Nalpas *et al.* 1995; Verweij & Simmelink 2002; Duin *et al.* 2016). In the Late Permian, the Northern and Southern Permian basins were submerged by the Zechstein Sea, which deposited >1-km-thick evaporites in the southern North Sea (Coward 1995). Subsequent continental rifting during the Triassic and Jurassic periods led to widespread subsidence and deposition of shallow- and deep-marine sediments, including thick shale sequences (Duin *et al.* 2016).

During the Cretaceous, thick sequences of chalk were deposited in the Broad Fourteens Basin, the exact

location of our 3D seismic volume (Verweij & Simmelink 2002), before a period of basin inversion associated with the Alpine Orogeny resulted in large-scale erosion (Nalpas *et al.* 1995; De Lugt *et al.* 2003). Continued basin inversion led to the formation of regional unconformities known to mark the Cretaceous–Tertiary boundary (De Lugt *et al.* 2003), the base of the Miocene (Oudmayer & de Jager 1993; Verweij & Simmelink 2002) and the Middle Miocene (Oudmayer & de Jager 1993; Wong *et al.* 2001).

Pelagic to hemipelagic claystones were deposited in the study area between the Palaeocene and the Middle Miocene (Wong *et al.* 2001). Subsequently, large deltas

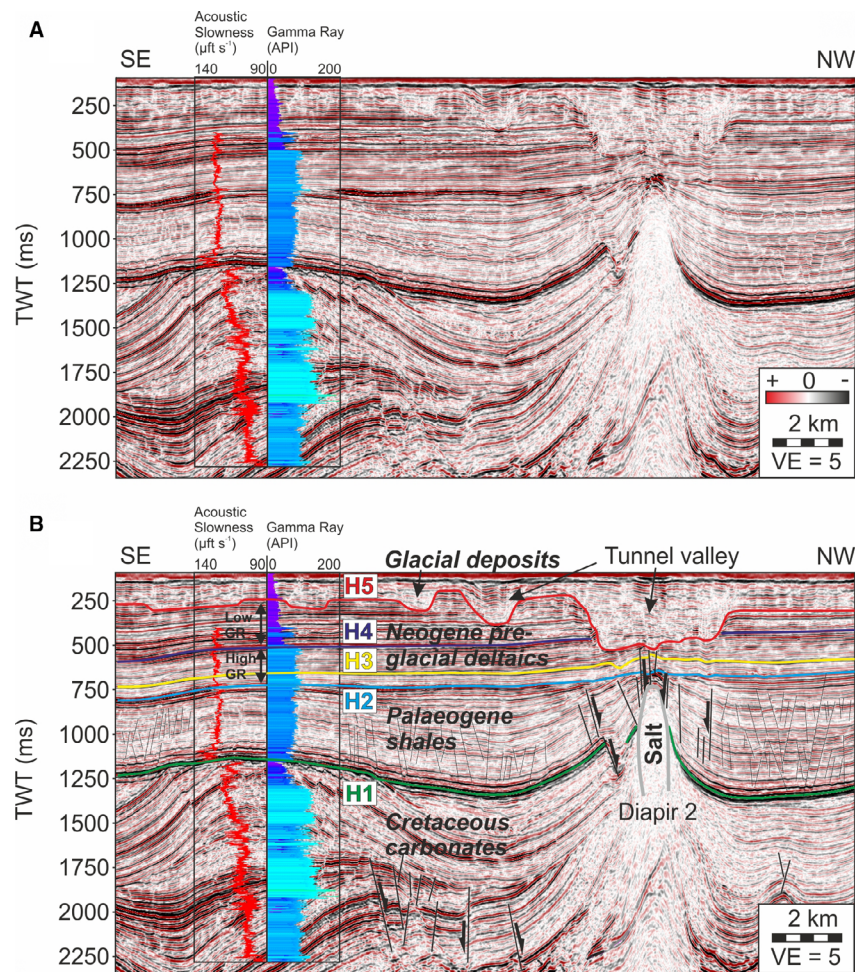


Fig. 3. A. Uninterpreted seismic profile across the study area showing Well K15-01 and corresponding acoustic slowness and gamma-ray curves (see Fig. 1 for location). B. Interpreted seismic profile imaging the same Well K15-01 and the seismic horizons interpreted in this work. Note the presence of the tunnel valley analysed in this work above horizon H5.

supplied by the palaeo-Rhine and the Baltic River System prograded onto the North Sea (Bijlsma 1981; Clausen *et al.* 1999; Overeem *et al.* 2001; Lamb *et al.* 2018). These deltas were either draped by shallow-marine sands or significantly eroded during Quaternary glacial–interglacial cycles (Huuse *et al.* 2001; Kuhlmann & Wong 2008).

Three major ice advances occurred in the North Sea during the Elsterian, Saalian and Weichselian glaciations (Ehlers 1990; Huuse & Lykke-Andersen 2000; Sejrup *et al.* 2000). Tunnel valleys are a widespread feature of these glacial periods (Huuse & Lykke-Andersen 2000; Praeg 2003; Passchier *et al.* 2010; Moreau *et al.* 2012; Van der Vegt *et al.* 2012). Ice fronts have been identified in the southern North Sea during the Elsterian and Saalian glaciations (Laban 1995; Praeg 1996; Gibbard *et al.* 2009; Moreau *et al.* 2012; Fig. 1). However, glaciers did not reach the study area during the Weichselian glaciation, between 115 000 and 11 700 years ago (Hughes *et al.* 2016) and did so only partially during the

Saalian glaciation, between ~300 000 and ~130 000 years ago (Fig. 1). Tunnel valleys in the Dutch sector of the North Sea, including the study area, are generally considered to be Elsterian in age, i.e. ranging from 500 000 to 410 000 years ago (Huuse & Lykke-Andersen 2000; Praeg 2003; Passchier *et al.* 2010; Moreau *et al.* 2012). Valley fills in the southern North Sea consist of glacial or postglacial fluvial to marine deposits, based on the analysis of seismic data (Moreau & Huuse 2014).

## Results

### *Cenozoic seismic stratigraphy*

In this study, we focus on the uppermost part of the sedimentary sequence filling the Broad Fourteens Basin, a part of the southern North Sea Basin that includes glacial Quaternary deposits and preglacial Palaeogene and Neogene strata (Fig. 2). Three distinct seismic units were identified as spanning the

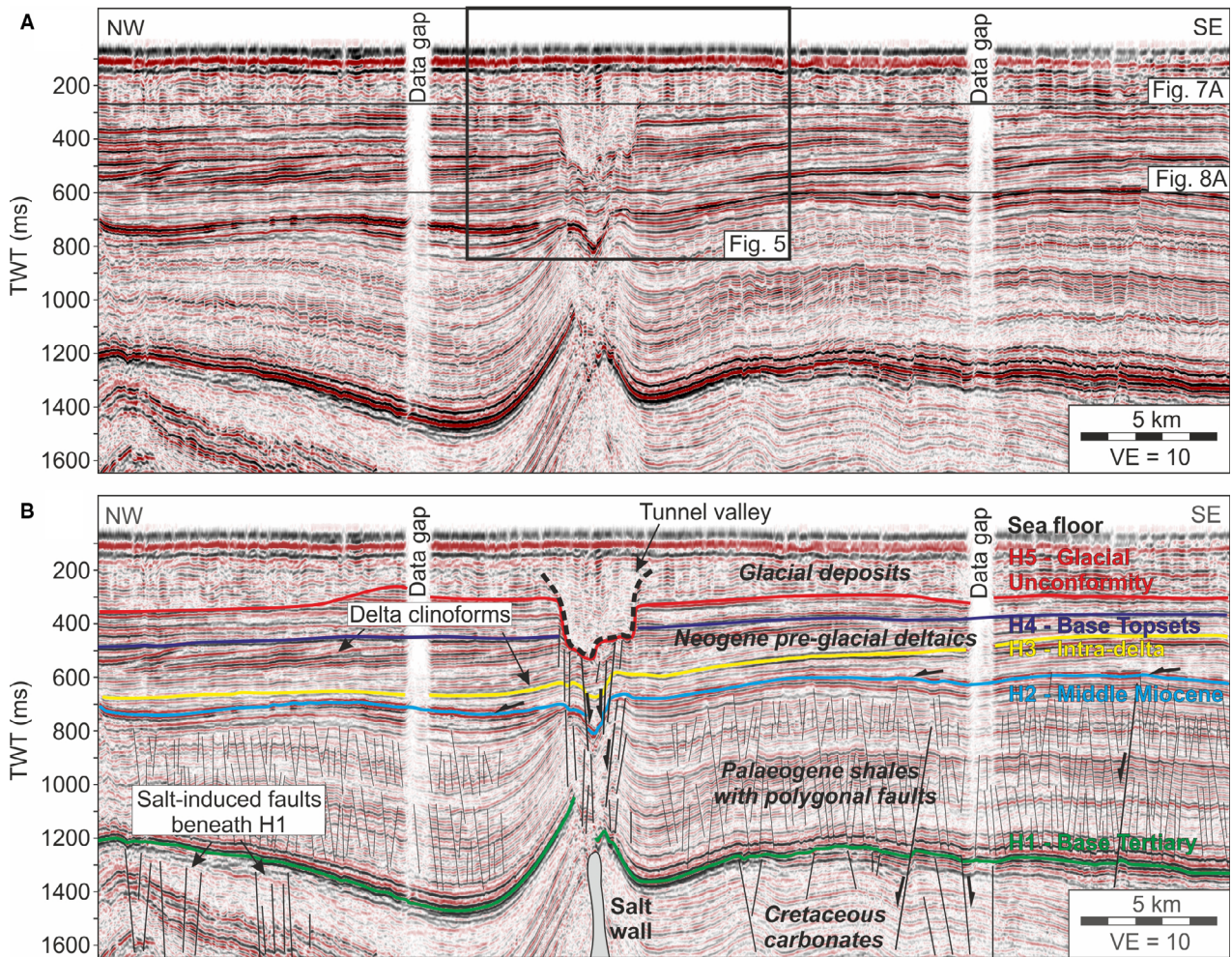


Fig. 4. Seismic profile showing the Cenozoic seismic stratigraphy, salt-induced faults and the glacial tunnel valley interpreted in this work (see Fig. 1 for location). A. Uninterpreted seismic profile. B. Interpreted seismic profile showing the mapped stratigraphical horizons in detail. Palaeogene shales with polygonal faults are overlain by Neogene deltaic deposits. Salt-induced faults occur primarily above the salt wall in the centre of the study area, leading to crestal faulting and local depocentres controlled by growth faults. Subglacial meltwater erosion incised the deltaic deposits and formed the large-scale tunnel valley.

geological evolution of the area during the Cenozoic. These units are bounded by prominent seismic reflectors that were mapped as distinct horizons in the 3D seismic volume (Figs 2, 3). The five interpreted horizons include, from top to bottom (Figs 2, 3): (i) the basal unconformity marking the onset of glaciation in the area (H5); (ii) the boundary between high-amplitude parallel delta topset reflections and underlying clinoform reflections (H4); (iii) a local unconformity of Neogene age amidst prograding deltaic deposits (H3); (iv) a Middle Miocene unconformity of regional extent (H2); and (v) the Base Tertiary Unconformity (H1).

Pre-Cenozoic strata include Permian continental units, Zechstein salt and Triassic to Cretaceous marine basin sediments (Ward *et al.* 2016). Strata underlying Cenozoic deposits show parallel moderate-amplitude

reflections in relatively thick Cretaceous carbonate sequences (Figs 3, 4).

#### *Palaeogene–Middle Miocene shales*

The base of Palaeogene strata is characterised by a prominent high-amplitude unconformity (H1) that truncates the underlying (Cretaceous) carbonates (Figs 2, 3). The upper boundary is characterised by a high-amplitude unconformity of Middle Miocene age (H2, Fig. 3) produced by regional uplift during the Alpine Orogeny (Cameron *et al.* 1993; Oudmayer & de Jager 1993; Wong *et al.* 2001).

Palaeogene strata show generally moderate-amplitude parallel internal reflections and an average thickness of ~600 ms TWT. Variations in thickness and reflection geometry occur around zones of salt-tectonic deformation, e.g. salt diapirs (Figs 2, 3). In addition,

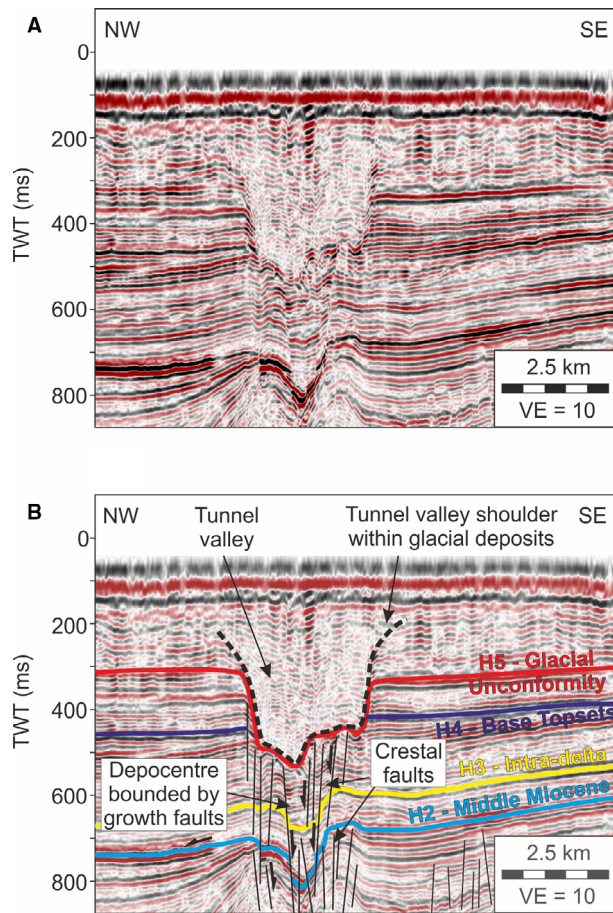


Fig. 5. A. Uninterpreted profile zoomed on the tunnel valley investigated in this work (see Fig. 2 for location). B. Interpreted profile of Fig. 5A. Crestal faults are extensional structures and extend onto the Glacial Unconformity (H5), i.e. the incision surface of the tunnel valley.

polygonal faults occur predominantly in areas not affected by intense salt-induced deformation (Fig. 4). As this unit correlates with Palaeogene and early Neogene claystones of the Lower and Middle North Sea group, deposited in pelagic to hemipelagic conditions (Wong *et al.* 2001), polygonal faults were likely formed due to dewatering during sediment compaction (Cartwright *et al.* 2003).

#### *Preglacial Neogene deltas*

Preglacial Neogene strata show moderate- to low-amplitude internal reflections that downlap onto the underlying Middle Miocene unconformity (H2, Figs 3, 4). This unit is approximately 300 ms TWT (~225 m) thick. Internally, clinoforms are observed in its lower part between H2 and H4, suggesting the deposition of deltaic prodelta and delta-front sediments. A mapped internal surface (H3) shows the shape of a clinoform reflector dipping gently towards the NW (Figs 4B, 5B). These clinoforms correlate with widespread deltaic

advance in the North Sea fed by the palaeo-Rhine and Baltic River Systems (Bijlsma 1981; Clausen *et al.* 1999; Overeem *et al.* 2001; Lamb *et al.* 2018; Ottesen *et al.* 2018; Patruno *et al.* 2020). Clinoforms are replaced by horizontal parallel reflections upwards and in the up-dip direction.

Horizon H4 marks the boundary between clinoforms associated with high gamma-ray values and horizontal reflections of increased amplitude with low gamma-ray values. The seismic reflections between H4 and H5 represent the topset parts of the Neogene preglacial delta deposits, i.e. relatively coarse-grained shallow-water sediments.

#### *Glacial deposits*

The shallowest deposits in the study area show low-amplitude parallel to chaotic reflections with a variable thickness of 100–500 ms TWT (75–375 m). The boundary between these glacial deposits and underlying preglacial deltaic strata is characterised by the prominent Glacial Unconformity H5 (Figs 3–6). Horizon H5 represents a regional unconformity in the southern and eastern North Sea (Nielsen *et al.* 2008; Moreau *et al.* 2012), contrasting with the conformable base of the Quaternary in the central North Sea (Lamb *et al.* 2018; Ottesen *et al.* 2018). Several elongated depressions within the Glacial Unconformity could be mapped to a depth of 570 ms TWT (~430 m) below the sea floor (Fig. 4). They show typical features of glacial tunnel valleys such as steep flanks, up to 300 m of erosion into underlying sediments, abrupt terminations, and a width of ~4 km (Figs 3–7).

The start and end of the major tunnel valley do not lie within the extent of the 3D seismic volume (Fig. 7). However, the same valley system was previously mapped and shows abrupt terminations to the north and south of the study area (Moreau *et al.* 2012). Secondary tunnel valleys show abrupt terminations, or onsets, within the 3D seismic volume (Fig. 7). Underlying reflections are clearly truncated by the valley flanks (Figs 4–6). The valley system shows generally a N–S orientation and a slightly meandering geometry (Fig. 7). The major tunnel valley is also characterised by multiple sills and local basins along its course (Fig. 7B). Several secondary valleys are connected to the dominant depression in the centre of the 3D seismic volume (Figs 6, 7).

#### *Salt-tectonic deformation of Cenozoic strata*

The study area shows extensive faulting due to salt-tectonic deformation. Most deformation occurs below H1 (Figs 4–6), whereas some faults penetrate as far as H2 (Figs 4B, 8A). Only the faults observed in the centre of the study area show activity throughout the Neogene to reach Horizon H5 (Fig. 4) and even affect shallow sediments close to the modern sea floor (Fig. 6).

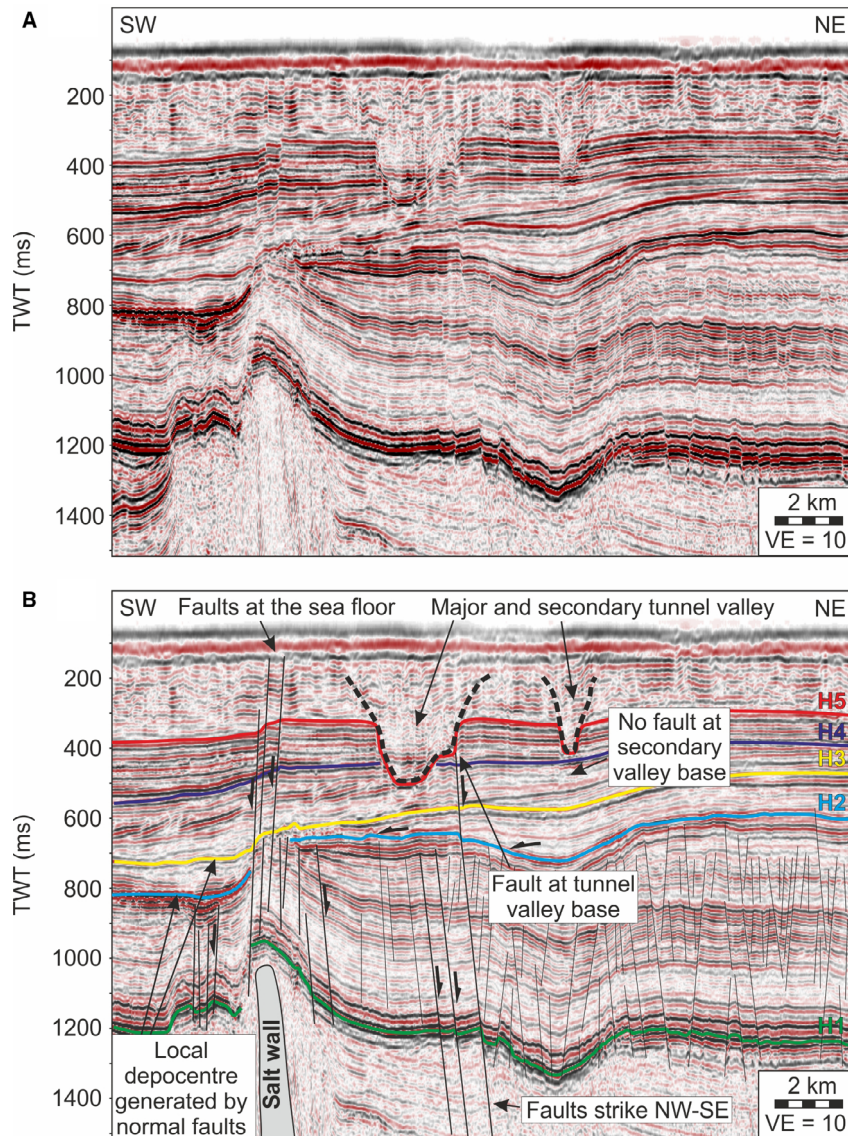


Fig. 6. A. Uninterpreted seismic profile imaging the southern part of the study area (see Fig. 1 for location). B. Interpreted seismic profile from Fig. 6A. Faults above the Zechstein salt wall affect Quaternary strata and may reach the sea floor. The major tunnel valley is located above NW–SE striking faults. These faults are not directly connected to the salt wall in the southern part of the study area. The secondary tunnel valley is not associated with salt-induced faulting.

Time slices through the interpreted 3D seismic volume show that individual faults have a limited lateral extent and arcuate geometries (Fig. 8A). The faulted region shows a general N–S strike (Fig. 8A), with normal faults predominating and forming relative depressions in the strata (Figs 5, 8B). Fault offsets and the depth of associated depressions decrease upwards along the faults when comparing H2 to H3, indicating growth faulting at depth (Fig. 5B).

The larger faults connect three individual salt diapirs (e.g. Fig. 3) developed along an elongated salt wall (Diapirs 1–3; Fig. 8A). At these diapir locations, salt has

risen from the Zechstein source layer at depth to the level of H2 (Fig. 3). The salt diapirs show locally intense faulting and morphological highs in mapped seismic reflectors (Fig. 8B). Between diapirs, the salt actually occurs much deeper, generally below H1 (Figs 4, 6).

Towards the south, some major faults show NW–SE strikes in the vicinity of Diapir 3, intersecting N–S crestal faults (Figs 6, 8). These NW–SE faults are rooted much deeper than the crestal faults with N–S strike (Fig. 6). In the south of the study area, horizons show a large-scale depression in association with salt-induced normal faults (Figs 6, 8B).

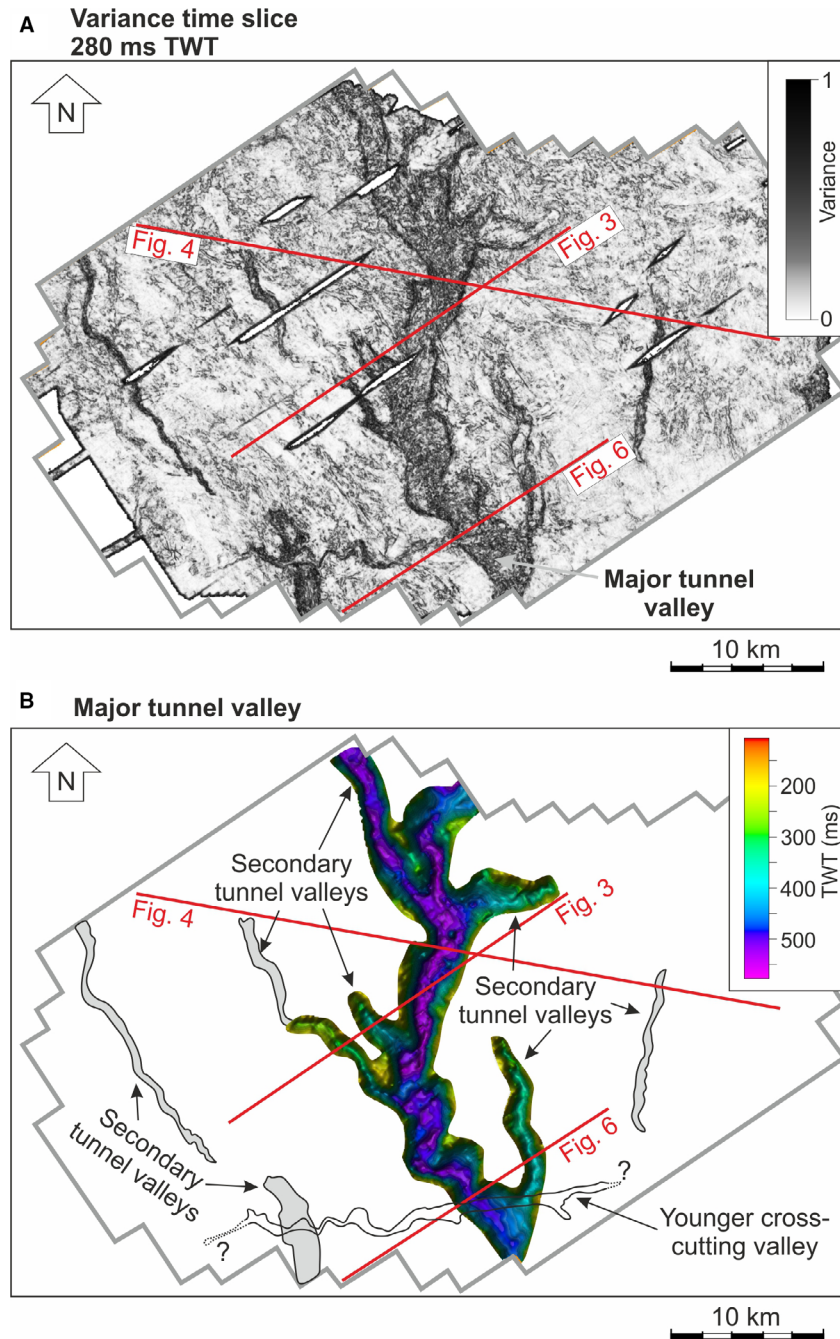


*Fig. 7.* A. Variance time slice at 280 ms TWT. This depth corresponds to the base of glacial deposits (Fig. 4). High-variance elongated areas correspond to valleys in glacial deposits. A major valley is present in the centre of the figure, together with secondary valleys. B. TWT structure of the major valley, showing ~350 ms TWT maximum vertical depth. Secondary valleys are also mapped in the figure based on the variance map in Fig. 7A. A cross-cutting valley in the southern part of the study area appears to be significantly younger.

## Discussion

### *Origin of tunnel valleys in the southern North Sea Basin*

In the study area, the mapped valleys coincide with the glacial tunnel valleys previously mapped at a broader scale by Huuse & Lykke-Andersen (2000), Praeg (2003), Kristensen *et al.* (2007) and Moreau *et al.*

(2012) (Fig. 7). Tunnel valleys are believed to be formed by different interacting processes, i.e. sediment liquefaction by overpressured subglacial meltwater and direct glacial erosion, requiring ice coverage of the area (Ó Cofaigh 1996; Huuse & Lykke-Andersen 2000; Jørgensen & Sandersen 2006; Janszen *et al.* 2012; Ravier *et al.* 2014). The valleys in our study area are likely Elsterian in age, as later glaciations did not reach

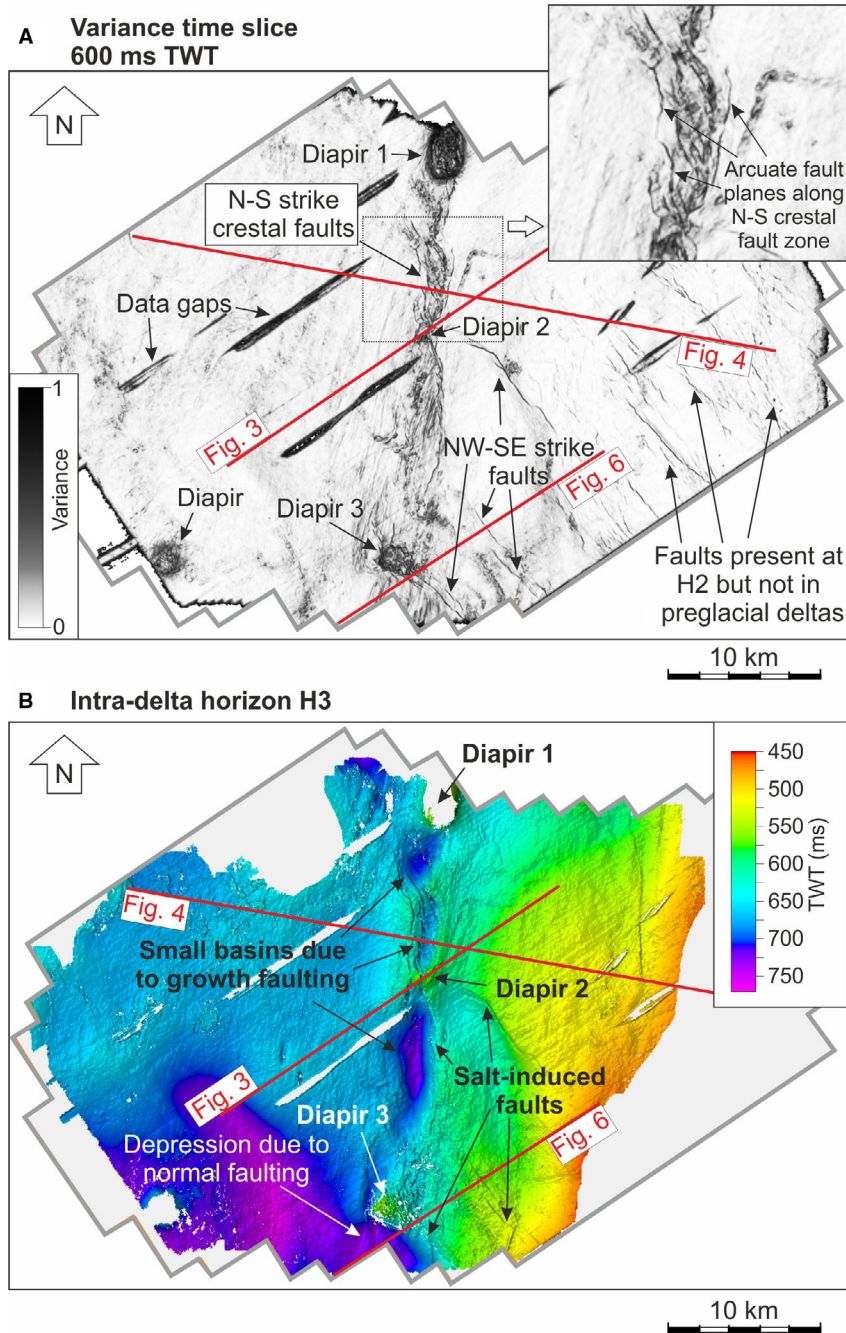


Fig. 8. A. Variance time slice at 600 ms TWT. This depth corresponds to preglacial deltas located directly underneath the major tunnel valley (see Fig. 4A). Semi-circular features of high variance correspond to salt diapirs, while linear high-variance features represent faults. Pervasive faulting can be observed between individual diapirs striking N–S in the centre of the data set. B. TWT structural map of the intra-delta surface (Horizon H3–Fig. 4B) showing morphological features of a surface directly underlying the tunnel valley. The crestal faults and small-scale depressions relate to salt-wall growth and are probably postdepositional in origin. A data acquisition footprint is visible as a faint SW–NE striping on time slices and shallow structural maps (see Marfurt & Alves 2015).

this location (Huuse & Lykke-Andersen 2000; Hughes *et al.* 2016). Nevertheless, the Saalian ice front was mapped in close proximity to the study area and we cannot exclude a Saalian age for the interpreted tunnel valleys (Fig. 1). Secondary tunnel valleys, as observed in our data (Fig. 7), are a common part of subglacial

drainage systems feeding into major meltwater pathways (Piotrowski 1997; Praeg 2003).

A secondary E–W striking valley in the south does not correspond to the overall N–S striking pattern of the main valleys interpreted in this work (Fig. 7). The N–S strike of the larger tunnel valleys was controlled by the

overall direction of ice flow, from north to south, as overpressured meltwater escaped along the steepest pressure gradient towards the ice front, located to the south of the study area during the Elsterian glaciation (Fig. 1; Moreau *et al.* 2012). Cross-cutting valleys are a typical feature of tunnel valley patterns in the North Sea and have been attributed to consecutive phases of ice coverage, either during the same glaciation or between individual major ice advances, and varying ice-front geometries (Kristensen *et al.* 2007; Stewart & Lonergan 2011; Stewart *et al.* 2013). In the study area, the E–W striking valley appears to be significantly younger than the major N–S striking tunnel valley, overlying the latter and not showing an interaction with observed faults (Fig. 7). Such a younger valley may either be a tunnel valley formed during later ice advances (e.g. Hepp *et al.* 2012), potentially during an ice advance of the Saalian glaciation that exceeded the mapped ice margin, or it may be a fluvial valley formed during subaerial exposure of the southern North Sea shelf during glacial periods (Fig. 1).

#### *Salt-induced faulting of Late Cenozoic strata*

Salt-tectonic activity of Zechstein salt in the North Sea has led to intense deformation of overlying Mesozoic and

Cenozoic strata (e.g. Verweij & Simmelink 2002; Stewart 2007; Arfai *et al.* 2018). However, salt-tectonic deformation of Cenozoic strata is relatively rare in the southern North Sea, as deformation affects predominantly pre-Palaeogene strata (Harding & Huuse 2015; Ward *et al.* 2016). In contrast to previous work, salt-induced faulting in the centre of the seismic volume clearly affects the entire Cenozoic succession (Figs 3–6, 8). These faults show activity throughout the Cenozoic and may even affect glacial deposits and reach the sea floor (Figs 4–6), as similarly reported from adjacent areas in the southern North Sea (Praeg 2003). In the study area, the latter faults are chiefly part of a crestal system developed above a N–S striking salt wall, a common occurrence in salt provinces (Stewart 2006; Figs 5, 8A). Their activity results in local depressions at the surface due to continued growth faulting, which is observed in the seismic horizons mapped along the salt wall (Figs 4–6, 8B). Continuous sedimentation filled these depressions to a large degree, simultaneously with their formation. Some deep-rooted faults occur in the southern half of the study area with a NW–SE strike (Fig. 6). These are related to fault blocks occurring close to the salt layer source (Ward *et al.* 2016).

The interpreted 3D seismic data have shown that the major tunnel valley running N–S directly overlies salt-

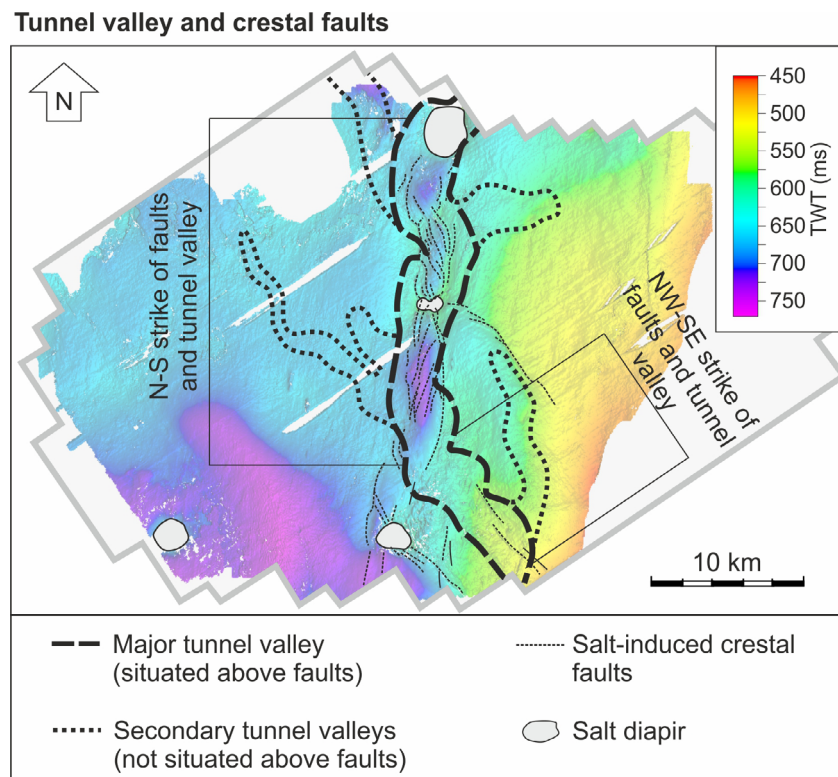


*Fig. 9.* Overlay of mapped crestal faults (Fig. 8) and tunnel valley outline (Fig. 7) on the TWT structural map of the mapped preglacial delta surface (Horizon H3). The glacial tunnel valley orientation follows pre-existing faults, overlying salt diapirs. Towards the south of the data set, the tunnel valley diverges southeastwards, potentially following faults striking in this direction. This coincidence between the course of the tunnel valley and crestal faulting is attributed to a decreased resistance to erosion of faulted surface sediments during tunnel valley formation.

induced crestal faults (Fig. 9). This tunnel valley crosses two diapirs along its course and deviates towards the SE in the south (Fig. 9). This deviation coincides with an intersection between N- and NW-striking faults in the southern part of the study area (Fig. 9).

#### *Tunnel valley formation along pre-existing faults*

The interpreted data allow us to consider three different processes to explain the formation of tunnel valleys in the study area. The first hypothesis considers the uplift–subsidence cycles that are typically recorded by crestal faults of rising diapirs (Vendeville & Jackson 1991; Mattos *et al.* 2016). Propagating sets of normal faults, associated with the crestal collapse of salt diapirs, could have formed surface depressions that guided ice and meltwater flow, and thus tunnel valley erosion. Importantly, salt diapirs were previously observed to influence the course of tunnel valleys (Piotrowski 1997; Kristensen *et al.* 2007). However, these latter studies generally report a diverting influence of salt diapirs, which is not the case in our study area as two salt diapirs are clearly overlaid by the major tunnel valley (Fig. 9). The southernmost Diapir 3 (Fig. 8) is not overlain by the tunnel valley (Fig. 9), possibly due to a shift in fault orientation towards the SE, diverting the tunnel valley away from the diapir (Fig. 6).

This discrepancy between the diversion of tunnel valleys from salt structures reported in the literature, and the occurrence of the larger tunnel valley over salt diapirs in our study area, may relate to the depth of salt occurrence. Salt diapirs only reach the Middle Miocene unconformity, likely limiting their control on tunnel valley formation compared to shallower occurrence of salt diapirs (Kristensen *et al.* 2007). Furthermore, the effect of pre-existing topography on the courses of tunnel valleys is minor in the study area as most salt-induced topography was filled by sediment during the main stages of crestal faulting, as illustrated at the level of H2 and H3 (Fig. 5). It is therefore probable that only minor surface topography existed at the onset of the Quaternary glaciations. Part of the major tunnel valley overlies the footwall of a deep-seated fault in the south of the study area (Fig. 6), suggesting a limited effect of substrate morphology on tunnel valley course.

A second hypothesis considers that sandy delta topsets were affected by salt-induced faults at the onset of the Quaternary glaciation, as documented by the faulted preglacial horizon H3 (Fig. 8B). As tunnel valleys are formed by subglacial meltwater erosion (Ó Cofaigh 1996; Huuse & Lykke-Andersen 2000; Jørgensen & Sandersen 2006), substrate resistance to such erosion determines the shapes and styles of tunnel valleys. This control of substrate geology on tunnel valley formation has previously been documented for different subglacial drainage features (Boulton *et al.* 2009; Moreau *et al.* 2012).

We suggest that the weakening of sediment by salt-induced crestal faults in the study area, and a relative decrease in its resistance to erosion, promoted the incision of a large tunnel valley along the crests of salt diapirs (Fig. 9). Subglacial erosion by meltwater would follow the areas of least resistance offered by faulted preglacial delta deposits. The orientation of the crestal faults approximately in the N–S direction coincides with the overall direction of the large tunnel valley, i.e. parallel to the ice advance (Fig. 1), and it facilitated erosion along the faulted sediments. Secondary small tunnel valleys (Fig. 7) do not coincide with the underlying structures; their formation appears thus not to be influenced by the zones of weakened sediment (Figs 8, 9). This may be due to the formation of a tunnel valley of substantial size along crestal faults, acting as a major subglacial dewatering pathway dominating the flow of subglacial meltwater in the area and leading to the formation of secondary tunnel valleys in its vicinity that fed meltwater to the major valley.

A third hypothesis considers a local dependence of tunnel valley formation on substrate geology. The major tunnel valley consistently truncates Horizon H4 (Figs 3–6). Sediments between H4 and H5 are interpreted as delta topset sediments, overlying clinofolds of Neogene delta complexes (Bijlsma 1981; Clausen *et al.* 1999; Overeem *et al.* 2001; Lamb *et al.* 2018). These sediments are probably coarse-grained, based on their relatively high seismic amplitude and their low gamma-ray values (Fig. 3). The underlying delta clinofolds between H2 and H4 show much higher gamma-ray values and lower seismic amplitudes (Fig. 3), hinting at the presence of finer grain sizes as expected in delta foreset clinofolds in comparison with their shallow water topsets. Substrate grain size and associated permeability have been reported as major factors controlling tunnel valley formation, with an increased occurrence of such valleys in areas of low permeability (Janszen *et al.* 2012; Sandersen & Jørgensen 2012). This has been attributed to the build-up of meltwater overpressure as water drainage through the sediment is limited and subsequent sediment liquefaction is promoted (Janszen *et al.* 2012; Sandersen & Jørgensen 2012). The relatively coarse-grained topset sediments in our study suggest a rather efficient subglacial meltwater flow through the sediment. However, subglacial meltwater drainage in these sediments may have been hampered by compaction through ice-loading, a more fine-grained sediment composition than expected, or simply by an excess of meltwater. In the absence of sufficient capacity for meltwater to percolate through the sediment, the crestal faults acted as pathways of increased permeability through delta-topset sediments, allowing the meltwater to reach low-permeability clinofold strata. Meltwater drainage would have been limited at this depth (below H4), leading to overpressure build-up and tunnel valley erosion along the fault planes.

Based on these three hypotheses, we favour a combined process in which the interpreted crestal faults led to the weakening of near-surface sediments at the start of the Quaternary glaciations, and constituted an efficient pathway for meltwater to flow deep into the substrate. Since the topset sediments did not provide sufficient drainage capacity, the subglacial meltwater followed the crestal faults downwards until it encountered the fine-grained clinoform deposits. The fine-grained sediment in the clinoforms did not allow a continued drainage of meltwater, possibly also reducing the permeability along crestal fault planes, leading to pressure build-up. In parallel, the weakening of topset sediments by salt-induced faulting probably facilitated the erosion of sediments along the fault zone, although we acknowledge that the erodibility of sediments depends on a wide range of parameters (Grabowski *et al.* 2011). Other tunnel valleys in the North Sea were offset by faults that continued to be active during and after tunnel valley formation but did not affect tunnel valley erosion (Praeg 2003). Interestingly, the coincidence between glacial erosion, tunnel valley formation and pre-existing faults has been noted in Ordovician examples (Ghienne *et al.* 2003) but not in more recent examples of fault-related tunnel valleys formed in the North Sea during the Quaternary glaciations. The influence of underlying faults on the courses of tunnel valleys will also depend on their orientation relative to the ice advance.

This work shows an apparent link amongst pre-existing fault systems and the orientation of tunnel valleys. However, the exact way(s) these interactions occurred in the past, i.e. whether tunnel valleys followed salt-induced structures or were diverted from them (e.g. Kristensen *et al.* 2007), probably depended on parameters such as the depth of salt and the geometry of complex families of diapir-related faults.

## Conclusions

This study interpreted a 3D seismic volume from the southern North Sea to reach the following conclusions:

- The course of a major tunnel valley in the southern North Sea coincides with salt-induced crestal faults above a Zechstein salt wall.
- Faulted sediments are expected to act as high-permeability pathways for meltwater to easily reach fine-grained clinoform deltaic sediments, resulting in the build-up of meltwater pressure and sediment liquefaction.
- Additionally, faulted sediments offer less resistance to erosion, facilitating tunnel valley formation. Hence, a change in tunnel valley orientation towards the SE correlates with a change in fault strike in the same direction.
- Salt diapirs reach strata as young as the Middle Miocene but do not divert the tunnel valley course, as

reported from other locations. This is probably due to the fact that salt is not shallow enough below the sea floor to directly affect tunnel valley formation.

- The smaller tunnel valleys in the area do not coincide with faults and were formed in non-weakened sediments. Their smaller sizes compared to the major tunnel valley suggest that they were formed as features secondary to the main meltwater discharge pathway.

Our study suggests that the pre-existing faults determined the strike and morphology of a major tunnel valley and subglacial dewatering pathways. In contrast, secondary tunnel valleys are not associated with faults. Tunnel valley formation during ice coverage of the area most likely occurred along these same fault zones as meltwater penetrated preglacial deltaic topset sediments along the faults. When reaching the underlying fine-grained deltaic clinoform deposits, drainage along the faults was hampered and water overpressure occurred, leading to sediment liquefaction and incision of tunnel valleys.

At present, tunnel valley courses in the North Sea region are not consistently regarded as governed by salt-induced faults and further work is needed to fully understand the control of salt structures on tunnel valleys in the region.

*Acknowledgements.* – This study was funded through the project ‘BoulderDetection’ (German Ministry of Economics and Energy (BMWi), project number 0324122B) and the Bremen-Cardiff-Alliance Collaborative Fund. Borehole data were provided by NLOG through its web repository. We thank Haloil for access and permission to publish examples from their 3D seismic data volume. Data are confidential and only available upon request to Haloil. Schlumberger is acknowledged for providing academic licences to Cardiff’s 3D Seismic Lab for the software package Petrel©. We also thank Boreas Editor-in-Chief J. A. Piotrowski as well as reviewers A. Janszen and M. Stewart for their constructive comments that have considerably improved the manuscript.

*Author contributions.* – SW carried out the main seismic data interpretation with support from TMA. The initial draft of the manuscript was prepared by SW. TMA provided comments and reviews of the manuscript and provided support for the preparation of figures.

## References

- Alves, T. M. & Elliott, C. 2014: Fluid flow during early compartmentalisation of rafts: a North Sea analogue for divergent continental margins. *Tectonophysics* 634, 91–96.
- Arfai, J., Franke, D., Lutz, R., Reinhardt, L., Kley, J. & Gaedicke, C. 2018: Rapid Quaternary subsidence in the northwestern German North Sea. *Scientific Reports* 8, 11524, <https://doi.org/10.1038/s41598-018-29638-6>.
- Bijlsma, S. 1981: Fluvial sedimentation from the Fennoscandian area into the Northwest European basin during the Late Cenozoic. *Geologie en Mijnbouw* 60, 337–345.
- Boulton, G. S., Hagdorn, M., Maillot, P. B. & Zatsepin, S. 2009: Drainage beneath ice sheets: groundwater–channel coupling, and the origin of esker systems from former ice sheets. *Quaternary Science Reviews* 28, 621–638.
- Cameron, T. D. J., Bulat, J. & Mesdag, C. S. 1993: High resolution seismic profile through a Late Cenozoic delta complex in the southern North Sea. *Marine and Petroleum Geology* 10, 591–599.

- Cartwright, J., James, D. & Bolton, A. 2003: The genesis of polygonal fault systems: a review. *Geological Society, London, Special Publications* 216, 223–243.
- Clausen, O. R., Gregersen, U., Michelsen, O. & Sørensen, J. C. 1999: Factors controlling the Cenozoic sequence development in the eastern parts of the North Sea. *Journal of the Geological Society* 156, 809–816.
- Coward, M. P. 1995: Structural and tectonic setting of the Permo-Triassic basins in northwest Europe. *Geological Society, London, Special Publications* 91, 7–39.
- Cutler, P. M., Colgan, P. M. & Mickelson, D. M. 2002: Sedimentologic evidence for outburst floods from the Laurentide Ice Sheet margin in Wisconsin, USA: implications for tunnel-channel formation. *Quaternary International* 90, 23–40.
- De Lugt, I. R., van Wees, J. D. & Wong, T. E. 2003: The tectonic evolution of the southern Dutch North Sea during the Palaeogene: basin inversion in distinct pulses. *Tectonophysics* 373, 141–159.
- Dobracki, R. & Krzyszkowski, D. 1997: Sedimentation and erosion at the Weichselian ice-marginal zone near Golczewo, Northwestern Poland. *Quaternary Science Reviews* 16, 721–740.
- Duin, E. J. T., Doornenbal, J. C., Rijkers, R. H. B., Verbeek, J. W. & Wong, T. E. 2016: Subsurface structure of the Netherlands - results of recent onshore and offshore mapping. *Netherlands Journal of Geosciences - Geologie en Mijnbouw* 85, 245–276.
- Ehlers, J. 1990: Reconstructing the dynamics of the North-west European Pleistocene ice sheets. *Quaternary Science Reviews* 9, 71–83.
- Ghienne, J.-F., Deynoux, M., Manatschal, G. & Rubino, J.-L. 2003: Palaeovalleys and fault-controlled depocentres in the Late-Ordovician glacial record of the Murzuq Basin (central Libya). *Comptes Rendus Geoscience* 335, 1091–1100.
- Gibbard, P. L., Pasanen, A. H., West, R. G., Lunkka, J. P., Boreham, S., Cohen, K. M. & Rolfé, C. 2009: Late Middle Pleistocene glaciation in East Anglia, England. *Boreas* 38, 504–528.
- Grabowski, R. C., Droppo, I. G. & Wharton, G. 2011: Erodibility of cohesive sediment: the importance of sediment properties. *Earth-Science Reviews* 105, 101–120.
- Harding, R. & Huuse, M. 2015: Salt on the move: multi stage evolution of salt diapirs in the Netherlands North Sea. *Marine and Petroleum Geology* 61, 39–55.
- Hepp, D. A., Hebbeln, D., Kreiter, S., Keil, H., Bathmann, C., Ehlers, J. & Mörz, T. 2012: An east–west-trending Quaternary tunnel valley in the south-eastern North Sea and its seismic–sedimentological interpretation. *Journal of Quaternary Science* 27, 844–853.
- Hughes, A. L. C., Gyllencreutz, R., Lohne, Ø. S., Mangerud, J. & Svendsen, J. I. 2016: The last Eurasian ice sheets – a chronological database and time-slice reconstruction, DATED-1. *Boreas* 45, 1–45.
- Huuse, M. & Lykke-Andersen, H. 2000: Overdeepened Quaternary valleys in the eastern Danish North Sea: morphology and origin. *Quaternary Science Reviews* 19, 1233–1253.
- Huuse, M., Lykke-Andersen, H. & Michelsen, O. 2001: Cenozoic evolution of the eastern Danish North Sea. *Marine Geology* 177, 243–269.
- Janszen, A., Spaak, M. & Moscariello, A. 2012: Effects of the substratum on the formation of glacial tunnel valleys: an example from the Middle Pleistocene of the southern North Sea Basin. *Boreas* 41, 629–643.
- Jørgensen, F. & Sandersen, P. B. E. 2006: Buried and open tunnel valleys in Denmark—erosion beneath multiple ice sheets. *Quaternary Science Reviews* 25, 1339–1363.
- Kehew, A. E., Piotrowski, J. A. & Jørgensen, F. 2012: Tunnel valleys: concepts and controversies—A review. *Earth-Science Reviews* 113, 33–58.
- Kristensen, T. B. & Huuse, M. 2012: Multistage erosion and infill of buried Pleistocene tunnel valleys and associated seismic velocity effects. *Geological Society, London, Special Publications* 368, 159–172.
- Kristensen, T. B., Huuse, M., Piotrowski, J. A. & Clausen, O. R. 2007: A morphometric analysis of tunnel valleys in the eastern North Sea based on 3D seismic data. *Journal of Quaternary Science* 22, 801–815.
- Kuhlmann, G. & Wong, T. E. 2008: Pliocene paleoenvironment evolution as interpreted from 3D-seismic data in the southern North Sea, Dutch offshore sector. *Marine and Petroleum Geology* 25, 173–189.
- Laban, C. 1995: *The Pleistocene glaciations in the Dutch sector of the North Sea: a synthesis of sedimentary and seismic data*. Ph.D. thesis, University of Amsterdam, 194 pp.
- Lamb, R. M., Harding, R., Huuse, M., Stewart, M. & Brocklehurst, S. H. 2018: The early Quaternary North Sea Basin. *Journal of the Geological Society* 175, 275–290.
- Lelandais, T., Mourgues, R., Ravier, É., Pochat, S., Strzeczynski, P. & Bourgeois, O. 2016: Experimental modeling of pressurized subglacial water flow: implications for tunnel valley formation. *Journal of Geophysical Research: Earth Surface* 121, 2022–2041.
- Marfurt, K. & Alves, T. M. 2015: Pitfalls and limitations in seismic attribute interpretation of tectonic features. *Interpretation* 3, SB5–SB15.
- Mattos, N. H., Alves, T. M. & Omosanya, K. 2016: Crestal fault geometries reveal late halokinesis and collapse of the Samson Dome, Northern Norway: implications for petroleum systems in the Barents Sea. *Tectonophysics* 690, 76–96.
- Moreau, J. & Huuse, M. 2014: Infill of tunnel valleys associated with landward-flowing ice sheets: the missing Middle Pleistocene record of the NW European rivers? *Geochemistry, Geophysics, Geosystems* 15, 1–9, <https://doi.org/10.1002/2013gc005007>.
- Moreau, J., Huuse, M., Janszen, A., van der Vegt, P., Gibbard, P. L. & Moscariello, A. 2012: The glaciogenic unconformity of the southern North Sea. *Geological Society, London, Special Publications* 368, 99–110.
- Nalpas, T., Le Douaran, S., Brun, J. P., Unternehr, P. & Richert, J. P. 1995: Inversion of the Broad Fourteens Basin (offshore Netherlands), a small-scale model investigation. *Sedimentary Geology* 95, 237–250.
- Nielsen, T., Mathiesen, A. & Bryde-Auken, M. 2008: Base Quaternary in the Danish parts of the North Sea and Skagerrak. *Geological Survey of Denmark and Greenland Bulletin* 15, 37–40.
- Ó Cofaigh, C. 1996: Tunnel valley genesis. *Progress in Physical Geography: Earth and Environment* 20, 1–19.
- Ottesen, D., Batchelor, C. L., Dowdeswell, J. A. & Løseth, H. 2018: Morphology and pattern of Quaternary sedimentation in the North Sea Basin (52–62°N). *Marine and Petroleum Geology* 98, 836–859.
- Oudmayer, B. C. & de Jager, J. 1993: Fault reactivation and oblique-slip in the Southern North Sea. *Geological Society, London, Petroleum Geology Conference Series* 4, 1281–1290.
- Overeem, I., Weltje, G. J., Bishop-Kay, C. & Kroonenberg, S. B. 2001: The Late Cenozoic Eridanos delta system in the Southern North Sea Basin: a climate signal in sediment supply? *Basin Research* 13, 293–312.
- Passchier, S., Laban, C., Mesdag, C. S. & Rijdsdijk, K. F. 2010: Subglacial bed conditions during Late Pleistocene glaciations and their impact on ice dynamics in the southern North Sea. *Boreas* 39, 633–647.
- Patrino, S., Scisciani, V., Helland-Hansen, W., D’Intino, N., Reid, W. & Pellegrini, C. 2020: Upslope-climbing shelf-edge clinofolds and the stepwise evolution of the northern European glaciation (lower Pleistocene Eridanos Delta system, U.K. North Sea): when sediment supply overwhelms accommodation. *Basin Research* 32, 224–239.
- Penge, J., Munns, J. W., Taylor, B. & Windle, T. M. F. 1999: Rift-raft tectonics: examples of gravitational tectonics from the Zechstein basins on northwest Europe. In Fleet, A. J. & Boldy, S. A. R. (eds.): *Petroleum Geology of Northwest Europe, Proceedings of the 5th Conference*, 201–213. Geological Society, London.
- Piotrowski, J. A. 1997: Subglacial hydrology in north-western Germany during the last glaciation: groundwater flow, tunnel valleys and hydrological cycles. *Quaternary Science Reviews* 16, 169–185.
- Praeg, D. 1996: *Morphology, stratigraphy and genesis of buried valleys in the southern North Sea basin*. Ph.D. thesis, University of Edinburgh, 207 pp.
- Praeg, D. 2003: Seismic imaging of mid-Pleistocene tunnel-valleys in the North Sea Basin—high resolution from low frequencies. *Journal of Applied Geophysics* 53, 273–298.

- Ravier, E., Buoncristiani, J.-F., Guiraud, M., Menzies, J., Clerc, S., Goupy, B. & Portier, E. 2014: Porewater pressure control on subglacial soft sediment remobilization and tunnel valley formation: a case study from the Alnif tunnel valley (Morocco). *Sedimentary Geology* 304, 71–95.
- Sandersen, P. B. E. & Jørgensen, F. 2012: Substratum control on tunnel-valley formation in Denmark. *Geological Society, London, Special Publications* 368, 145–157.
- Sejrup, H. P., Larsen, E., Landvik, J., King, E. L., Haflidason, H. & Nesje, A. 2000: Quaternary glaciations in southern Fennoscandia: evidence from southwestern Norway and the northern North Sea region. *Quaternary Science Reviews* 19, 667–685.
- Stewart, S. A. 2006: Implications of passive salt diapir kinematics for reservoir segmentation by radial and concentric faults. *Marine and Petroleum Geology* 23, 843–853.
- Stewart, S. A. 2007: Salt tectonics in the North Sea Basin: a structural template for seismic interpreters. In Ries, A. C., Butler, R. W. & Graham, R. H. (eds.): *Deformation of the Continental Crust: The Legacy of Mike Coward*, 361–396. *Geological Society of London, Special Publications* 272.
- Stewart, M. A. & Lonergan, L. 2011: Seven glacial cycles in the middle-late Pleistocene of northwest Europe: geomorphic evidence from buried tunnel valleys. *Geology* 39, 283–286.
- Stewart, M., Lonergan, L. & Hampson, G. 2012: 3D seismic analysis of buried tunnel valleys in the Central North Sea: tunnel valley fill sedimentary architecture. *Geological Society, London, Special Publications* 368, 173–184.
- Stewart, M. A., Lonergan, L. & Hampson, G. 2013: 3D seismic analysis of buried tunnel valleys in the central North Sea: morphology, cross-cutting generations and glacial history. *Quaternary Science Reviews* 72, 1–17.
- Van der Vegt, P., Janszen, A. & Moscariello, A. 2012: Tunnel valleys: current knowledge and future perspectives. *Geological Society, London, Special Publications* 368, 75–97.
- Van Wijhe, D. H. 1987: Structural evolution of inverted basins in the Dutch offshore. *Tectonophysics* 137, 171–219.
- Vendeville, B. C. & Jackson, M. P. 1991: The rise of diapirs during thin-skinned extension. *Marine and Petroleum Geology* 9, 331–354.
- Verweij, J. M. & Simmelink, H. J. 2002: Geodynamic and hydrodynamic evolution of the Broad Fourteens Basin (The Netherlands) in relation to its petroleum systems. *Marine and Petroleum Geology* 19, 339–359.
- Ward, N. I. P., Alves, T. M. & Blenkinsop, T. G. 2016: Reservoir leakage along concentric faults in the Southern North Sea: implications for the deployment of CCS and EOR techniques. *Tectonophysics* 690, 97–116.
- Wong, T. E., Parker, N. & Horst, P. 2001: Tertiary sedimentary development of the Broad Fourteens area, the Netherlands. *Netherlands Journal of Geosciences - Geologie en Mijnbouw* 80, 85–94.